catalysts

MDPI

Article

Oxidative Bio-Desulfurization by Nanostructured Peroxidase Mediator System

Eliana Capecchi [1,*], Davide Piccinino [1], Bruno Mattia Bizzarri [1], Lorenzo Botta [1], Marcello Crucianelli [2] and Raffaele Saladino [1,*]

[1] Department of Biological and Ecological Sciences, University of Tuscia, Via S. Camillo de Lellis snc, 01100 Viterbo, Italy; d.piccinino@unitus.it (D.P); bm.bizzarri@unitus.it (B.M.B); lorenzo.botta@unitus.it (L.B.)

[2] Department of Physical and Chemical Sciences, University of L'Aquila, Via Vetoio I, Coppito, 67100 L'Aquila, Italy; marcello.crucianelli@univaq.it

* Correspondence: e.capecchi@unitus.it (E.C.); saladino@unitus.it (R.S.)

Received: 21 February 2020; Accepted: 6 March 2020; Published: 9 March 2020

Abstract: Bio-desulfurization is an efficient technology for removing recalcitrant sulfur derivatives from liquid fuel oil in environmentally friendly experimental conditions. In this context, the development of heterogeneous bio-nanocatalysts is of great relevance to improve the performance of the process. Here we report that lignin nanoparticles functionalized with concanavalin A are a renewable and efficient platform for the layer-by-layer immobilization of horseradish peroxidase. The novel bio-nanocatalysts were applied for the oxidation of dibenzothiophene as a well-recognized model of the recalcitrant sulfur derivative. The reactions were performed with hydrogen peroxide as a green primary oxidant in the biphasic system PBS/*n*-hexane at 45 °C and room pressure, the highest conversion of the substrate occurring in the presence of cationic polyelectrolyte layer and hydroxy-benzotriazole as a low molecular weight redox mediator. The catalytic activity was retained for more transformations highlighting the beneficial effect of the support in the reusability of the heterogeneous system.

Keywords: oxidative bio-desulfurization; lignin nanoparticles; horseradish peroxidase; dibenzothiophene

1. Introduction

Many efforts are devoted to removing recalcitrant aromatic sulfur compounds from liquid fuel oil, as a consequence of the application of the international legislation for the protection of the environment from the emission of sulfur oxides [1]. Among new technologies, oxidative desulfurization (ODS) [2,3] has gained growing interest thanks to the development of selective and efficient catalytic procedures for the extraction of sulfur contaminants, even when they are present in the liquid fuel oil in a very low amount [4]. Analysis and review of the application of metal-based heterogeneous nano-catalysts in ODS procedures [5–8], as well as the role played by different primary oxidants in the desulfurization process [9,10], are reported in the literature [11], hydrogen peroxide (H_2O_2) emerging as a well-recognized green reagent [12,13]. As an alternative, H_2O_2 and dioxygen can be activated in bio-desulfurization processes by use of microorganisms [14–16] or crude and purified enzymes, including laccase [17], laccase mediator system (LMS) [18], hemoglobin [19], lignin peroxidase [20], manganese peroxidase [21], microperoxidase-1 [22], chloroperoxidase [23], lactoperoxidase [24] and horseradish peroxidase [25,26] assisted by ultrasound treatment [27]. These procedures avoid the leaching of active species from metal oxides and organometallic reagents and are effective at low pressure and temperature in a large range of pH values [28]. Moreover, the use of enzymes makes the overall treatment greener.

Despite the efforts to optimize the efficacy of bio-desulfurization processes, only a few examples of immobilization protocols are reported, limited to the use of mesoporous Santa Barbara Amorphous silica SBA-16 and zeolite Al-MCM-41 [29], sol-gel supports [30] at the micro-scale and single-walled carbon nanotubes [31] and (1D)-γ-Al_2O_3 nanorods [32] at the nano-scale. The immobilization of enzymes is of practical relevance since it reduces the protein denaturation and improves activity, stability and selectivity, favoring the use of the bio-catalyst for more treatments [33].

Recently, we reported that nanoparticles of lignin (LNPs), the most abundant polyphenol in nature [34], show improved antioxidant and UV-absorbing properties. LNPs are easily obtained by the layer-by-layer technology [35], and used as a renewable platform for the immobilization of oxidative enzymes, such as laccase [36] and tyrosinase [37]. In particular, LNPs showed specific boosting activity for laccase by long-range electron transfer (pseudo-DET) and mediated electron transfer (MET) mechanisms between the structurally oriented aromatic groups in the polymer and the enzyme [38]. In a similar way, the boosting activity of lignin was operative in the monooxygenase mediated oxidative degradation of polyphenols by formation of low molecular weight lignan fragments able to perform as bulk diffusible redox mediators [39,40]. In order to further improve nano-catalysis in bio-desulfurization processes, we report here the immobilization of horseradish peroxidase (HRP) on LNPs by the layer-by-layer procedure and the application of the novel nano-biocatalysts in the H_2O_2 oxidation of dibenzothiophene (DBT) as a well-recognized model of ODS. The use of concanavalin A (Con A) for the controlled orientation of HRP on the surface of LNPs [41], associated to the presence of a multiple layered structure of cationic polyelectrolytes poly(diallyl-dimethylammonium chloride) PDDA and cationic lignin CATLIG, were found to be crucial elements for the optimal removal of DBT.

2. Results and Discussion

2.1. Preparation of Nanobiocatalysts

LNPs were prepared starting from two raw polyphenols with different hydrophobicity organosolv lignin (OL) [42] and kraft lignin (KL) [43] by use of the nanoprecipitation procedure [44]. The immobilization of HRP on OL-LNPs and KL-LNPs is schematically represented in Scheme 1.

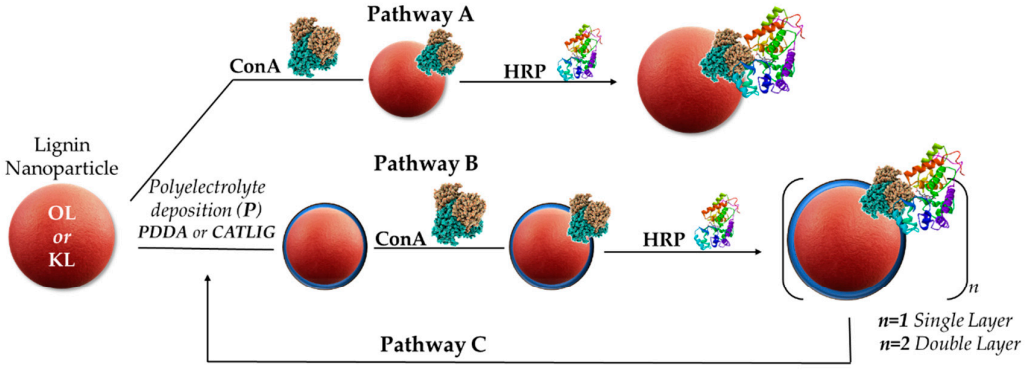

n	P	OL	KL
-	-	**Cat I**	**Cat II**
1	PDDA	**Cat III**	**Cat V**
1	CATLIG	**Cat IV**	**Cat VI**
2	PDDA	**Cat VII**	**Cat IX**
2	CATLIG	**Cat VIII**	**Cat X**

Scheme 1. Preparation of biocatalysts **I-X**. Pathway A: Direct adsorption of Con A on nanoparticles of lignin (LNPs) followed by immobilization of horseradish peroxidase (HRP). Pathway B: Layer-by-layer mediated adsorption of Con A; n is the number of layers and P indicates the type of cationic polyelectrolyte. Pathway C: Repeated cycle of deposition of the polyelectrolyte, Con A and HRP.

The site-specific immobilization and spatial orientation of HRP on the surface of the support is an essential parameter to avoid the random distribution of the enzyme, which is responsible for undesired conformational modification and shielding of the active site [45]. Con A, a homo-tetramer protein with ζ-potential of −14 mV [46] and specific molecular recognition properties for glycoproteins, selectively recognize HRP preserving the enzyme from denaturation [47]. On the basis of these data, OL-LNPs and KL-LNPs were functionalized with Con A and successively loaded with HRP [41]. Briefly, the appropriate LNPs (1.5 mg) dispersed in buffer (1.0 mL; 0.1 M PBS, pH 7.3) were treated with a freshly prepared PBS solution of Con A (0.5 mg/mL) followed by the addition of HRP (18 units) at 5 °C to yield OL-Con A/HRP **cat I** and KL-Con A/HRP **cat II** (Scheme 1, Pathway A). The effective loading of Con A on OL-LNPs and KL-LNPs was confirmed by the presence of the FT-IR vibrational mode at c.a. 1644 cm^{-1} corresponding to the amide I (C=O) band characteristic of the Con A structure (Figure 1) [48]. Furthermore, the formation of the complex between immobilized Con A and HRP was detected by confocal analysis of **cat I** as representative sample after the fluorescein isothiocyanate (FITC) labeling (Figure 2. Panel A: HRP showed a green fluorescence signal; Panel B: Magnification of the emission sites).

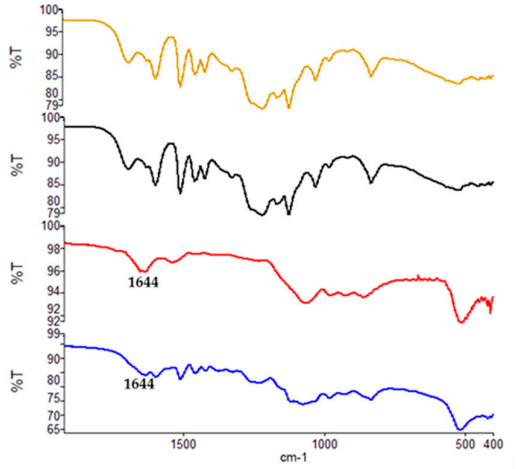

Figure 1. FT-IR analysis of Con A after deposition on organosolv lignin (OL)-LNPs (red line) and kraft lignin (KL)-LNPs (blue line). The FT-IR spectra of native OL-LNPs and KL-LNPs (yellow line and black line) are reported as references. The amide I (C=O) stretching band typical of the Con A structure is located at c.a. 1644 cm^{-1}.

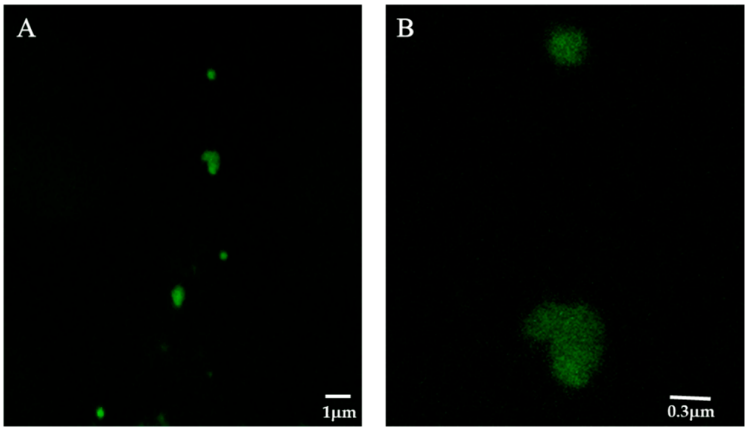

Figure 2. Confocal image of **cat I** (Panel **A**) after fluorescein isothiocyanate (FITC) labeling and magnification of the emission site (Panel **B**).

As an alternative, Con A was adsorbed on OL-LNPs and KL-LNPs after the initial deposition of a cationic polyelectrolyte layer of PDDA or CATLIG. In this latter case LNPs (1.5 mg) dispersed in buffer (1.0 mL; 0.1 M PBS, pH 7.3) were coated with the appropriate polyelectrolyte [38] followed by treatment with PBS solution of Con A (0.5 mg/mL) and addition of HRP (18 units) to yield OL-PDDA-ConA/HRP **cat III**, OL-CATLIG-ConA/HRP **cat IV**, KL-PDDA-ConA/HRP **cat V** and KL-CATLIG-ConA/HRP **cat VI** (Scheme I, Pathway B). The procedure was repeated under similar experimental conditions for the deposition of a second layer of polyelectrolyte, Con A and HRP, to afford OL-(PDDA-ConA/HRP)$_2$ **cat VII**, OL-(CATLIG-ConA/HRP)$_2$ **cat VIII**, KL-(PDDA-ConA/HRP)$_2$ **cat IX** and KL-(CATLIG-ConA/HRP)$_2$ **cat X** (Scheme I, Pathway C). The morphological characterization of **cat I-X** performed by Scanning Electron Microscopy (SEM) analysis is reported in Figures 3 and 4, respectively. Irrespective from the experimental conditions, the LNPs retained their original regular spherical shape after the deposition procedure. Note that the surface of biocatalysts is characterized by a corona-like structural motif that is reported to be characteristic for the deposition of Con A [49].

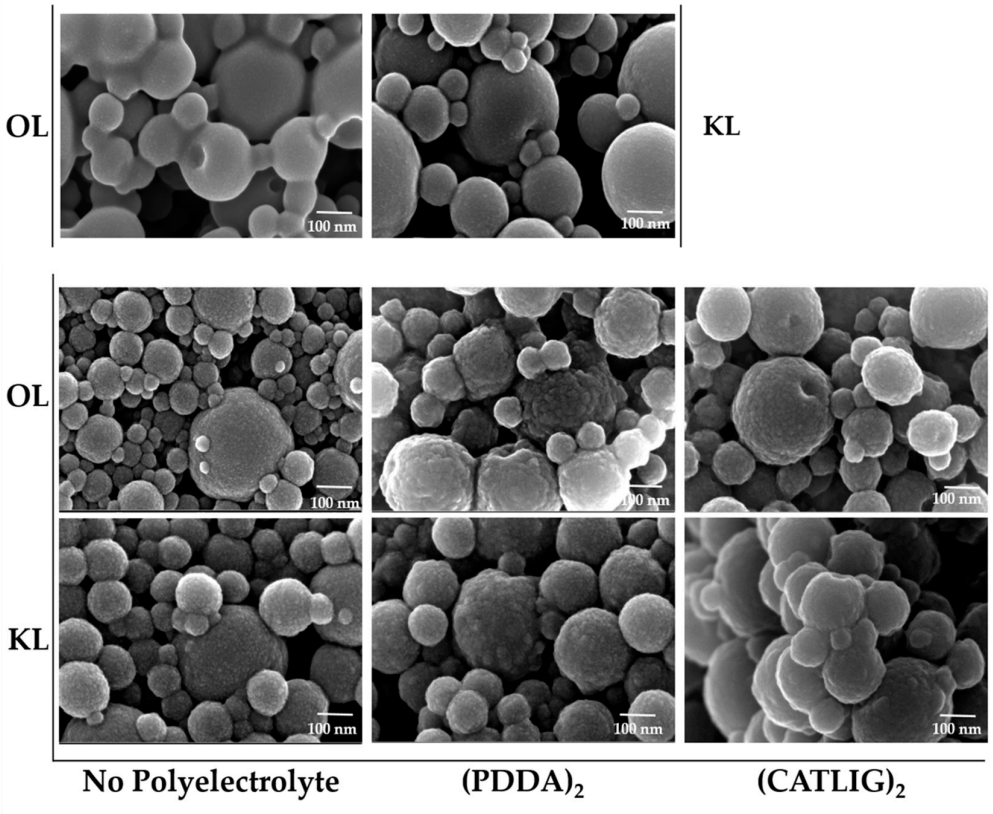

Figure 3. Upper panel: Scanning Electron Microscopy (SEM) images of OL-LNPs and KL-LNPs. Lower panel: SEM images of **cat I-II** and **cat VII-X**, separately. The n index in subscript of the parenthesis represents the number of cyclic depositions of polyelectrolyte, Con A and HRP. The corona-like motif present on the surface of nanoparticles is characteristic of the deposition of Con A as the external layer.

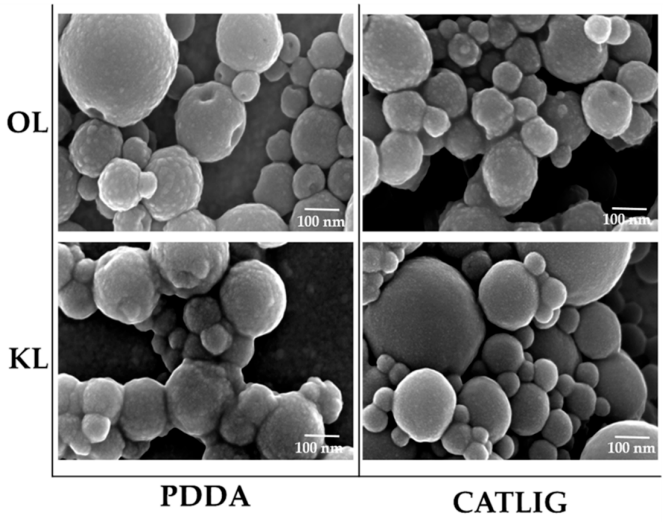

Figure 4. Upper panel: SEM images of **cat III-IV**. Lower panel: SEM images of **cat V-VI**.

2.2. Activity Parameters and Kinetic Data of Biocatalysts I–X

The activity parameters of **cat I–X** were measured through the standard 2,2′-azinobis-(3-ethylbenzothiazoline-6-sulfonic acid) (ABTS) test [50], consisting in the detection of the ABTS cation radical at 415 nm (ε420 = 36 000 M^{-1} cm^{-1}). The activity, activity yield and immobilization yield were determined using Equations 1–3, respectively:

$$\text{Activity (units per mg)} = U_x/W_{support} \quad (1)$$

$$\text{Activity yield (\%)} = [U_x/(U_a - U_r)] \times 100 \quad (2)$$

$$\text{Immobilization yield (\%)} = [(U_a - U_r)/U_a] \times 100 \quad (3)$$

Where U_a is the total activity (units) of HRP, U_r is the residual activity (units) in the solution and U_x is the activity of HRP after immobilization (the enzyme unit is the increase in the absorbance of 10^{-3} unit per min at 25 °C in 0.1 M Na-acetate buffer, pH 5). The presence of the cationic polyelectrolyte layer favors the immobilization yield of Con A/HRP on LNPs, PDDA and CATLIG showing a similar efficacy (Table 1, entries 3–4 and 7–8 versus entries 5–6 and 9–10). Moreover, the immobilization yield was increased by increasing the total number of layers. The activity yield of HRP was found to be dependent on the specific nature of LNPs in the absence of polyelectrolyte. **Cat I** showed an activity yield significantly lower than **cat II** (Table 1, entry 1 versus entry 2), suggesting that the different hydrophobicity and elemental composition of OL with respect to KL was a relevant parameter in tuning the efficacy of the Con A immobilization, probably due to dissociation of its dimeric sub-units [51]. This hypothesis is in accordance with the reported hydrophilicity character of Con A layers [52]. The presence of PDDA and CATLIG generally increased the activity yield, the overall effect being more pronounced in the case of OL (Table 1, entry 1 versus entries 3–4) relative to KL (Table 1, entry 2, versus entries 5–6). As a general trend, the activity yield was increased by increasing the number of the total layers, KL based biocatalysts being generally the most active systems (Table 1, entries 9-10 versus entries 5–6).

Table 1. Activity parameters and kinetic data of **cat I–X**. [1.]

Entry	Lignin/P	Cat	Immobilization Yield%	Activity Yield %	Activity (U/mg)	K_m (mM)	V_{max} (μM/s)
1	OL	**I**	45	21	3.78	12.5	0.26

2	KL	**II**	53	63	11.34	11.3	0.28
3	OL/PDDA	**III**	56	43	7.74	9.9	0.30
4	OL/CATLIG	**IV**	57	64	11.52	9.7	0.33
5	KL/PDDA	**V**	62	72	12.96	9.8	0.32
6	KL/CATLIG	**VI**	64	86	15.48	9.4	0.34
7	OL/$(PDDA)_2$	**VII**	68	75	13.50	8.3	0.34
8	OL/$(CATLIG)_2$	**VIII**	69	76	13.68	8.1	0.36
9	KL/$(PDDA)_2$	**IX**	72	84	15.12	8.2	0.34
10	KL/$(CATLIG)_2$	**X**	73	85	15.30	7.9	0.35
11	None	**HRP**	-	-	18.00	9.5	0.35

[1] ABTS in the range of 0.3–20 mM. Data were elaborated by a double reciprocal Lineweaver–Burk plot. The experiments were carried out in triplicate. Average errors in kinetic parameters were 2–4% for K_m and 1–3% for V_{max}.

Kinetic parameters of **cat I–X** are reported in Table 1 (entries 1–10), using native HRP as a reference (Table 1, entry 11). The biocatalyst carrying out the cationic polyelectrolyte layer showed K_m and V_{max} values comparable to that of native HRP irrespective from the lignin type (Table 1, entries 3–10 versus entry 11). In this latter case, the systems coated with PDDA where characterized by K_m and V_{max} values slightly higher than that measured for the CATLIG counterpart. Moreover, the K_m values decreased (and V_{max} increased) by increasing the total number of the layers (Table 1, entries 7–10 versus entries 3–6) [53]. In the absence of the cationic polyelectrolyte higher value of K_m were always observed (Table 1, entries 1–2). Other supports showed a similar trend, [54] indicating a reduction of the catalytic efficiency due to mass transfer limitation processes [55] and restriction of the mobility of the enzyme [56].

2.3. Oxidation of DBT with cat I–X

As a general procedure, DBT (10 mg, 0.05 mmol) and the appropriate biocatalyst (18 U/mg) in *n*-hexane (4 mL) and phosphate buffer saline PBS (0.1M pH 8, 4mL) were treated with H_2O_2 (4.0 equiv) at 45 °C for 2 h. The addition of the primary oxidant was performed in more steps to avoid the inactivation of HRP. [26] In alternative, hydroxybenzotriazole HoBt (20 µg, 1.0×10^{-3} mmol) and veratryl alcohol VA (18 µg, 1.0×10^{-3} mmol) were used as redox mediators. Low molecular weight redox mediators are electron shuttles for the peroxidase [57], showing beneficial effect on the overall catalytic activity [58]. HoBt and VA have a similar mechanism for the redox transfer process, encompassing the radical hydrogen abstraction (HAT) pathway [50]. The oxidation with native HRP and with H_2O_2 in the absence of the enzyme were performed as references. No oxidation of DBT occurred without the enzyme. Irrespective from the experimental conditions, the reaction was very selective to yield the dibenzothiophene sulfone (DBTO) as the only recovered product (Table 2).

Table 2. Application of **cat I-X** in the oxidation of dibenzothiophene (DBT) as a model of oxidative desulfurization (ODS).

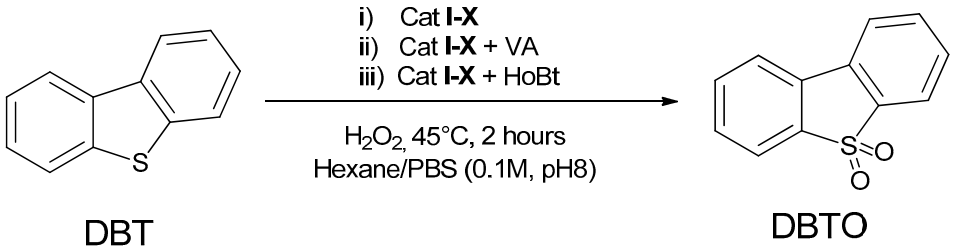

Entry	Lignin/P	Cat	Redox Mediator [1]	Conversion (%)	Yield (%) [2]
1	OL	**I**	none	18	>99
2	KL	**II**	none	22	>99

3	OL/PDDA	**III**	none	20	>99
4	OL/CATLIG	**IV**	none	23	>99
5	KL/PDDA	**V**	none	30	>99
6	KL/CATLIG	**VI**	none	32	>99
7	OL/$(PDDA)_2$	**VII**	none	35	>99
8	OL/$(CATLIG)_2$	**VIII**	none	36	>99
9	KL/$(PDDA)_2$	**IX**	none	37	>99
10	KL/$(CATLIG)_2$	**X**	none	38	>99
11	None	**HRP**	none	78	>99
12	OL	**I**	VA	25	>99
13	OL	**I**	HoBt	34	>99
14	KL	**II**	VA	32	>99
15	KL	**II**	HoBt	46	>99
15	OL/PDDA	**III**	VA	28	>99
17	OL/PDDA	**III**	HoBt	33	>99
18	OL/CATLIG	**IV**	VA	31	>99
19	OL/CATLIG	**IV**	HoBt	36	>99
20	KL/PDDA	**V**	VA	43	>99
21	KL/PDDA	**V**	HoBt	52	>99
22	KL/CATLIG	**VI**	VA	44	>99
23	KL/CATLIG	**VI**	HoBt	53	>99
24	$OL(PDDA)_2$	**VII**	VA	54	>99
25	$OL(PDDA)_2$	**VII**	HoBt	64	>99
26	$OL(CATLIG)_2$	**VIII**	VA	55	>99
27	$OL(CATLIG)_2$	**VIII**	HoBt	65	>99
28	$KL(PDDA)_2$	**IX**	VA	53	>99
29	$KL(PDDA)_2$	**IX**	HoBt	64	>99
30	$KL(CATLIG)_2$	**X**	VA	54	>99
31	$KL(CATLIG)_2$	**X**	HoBt	65	>99
32	$KL(CATLIG)_2$	**X**	HoBt	64 (Run no.1)[3]	>99
33	$KL(CATLIG)_2$	**X**	HoBt	60 (Run no.2)	>99
34	$KL(CATLIG)_2$	**X**	HoBt	58 (Run no.3)	>99
35	$KL(CATLIG)_2$	**X**	HoBt	42 (Run no.4)	>99
36	$KL(CATLIG)_2$	**X**	HoBt	45 (Run no.5)	>99
37	None	**HRP**	VA	55	>99
38	None	**HRP**	HoBt	70	>99

[1] **Cat I-X** (18 U/mg of HRP), 4.0 equiv. of H_2O_2, n-hexane, PBS (0.1 M, pH 8) with two redox mediators: Veratryl alcohol (VA) and 1-Hydroxybenzotriazole (HoBt) at 45 °C. [2] The yield is referred to converted substrate. [3] **Cat X** was recovered by centrifugation and used in the following runs.

The conversion of DBT with **cat I-X** was lower than that obtained with HRP in the absence of the redox mediators, probably as a consequence of the occurrence of mass-transfer limitation processes associated to the heterogeneous system. Double layered systems **cat VII-X** were the most effective biocatalysts irrespective from the lignin type and the nature of the polyelectrolyte layer. In this latter case, conversion values in the range of 35–38% were observed (Table 2, entries 6–10). Better results were obtained using the redox mediators (38–65% conversion range), HoBt performing better than VA. This different behavior is probably due to the reported lower redox-potential value of HoBt with respect to VA, favoring the oxidation of the substrate [59]. The conversion of DBT with double layered **cat VII-X** was of the same order of magnitude as that obtained with HRP and both VA and HoBt (Table 2, entries 24–31 versus entries 37–38). The efficacy of the KL based biocatalysts was higher than the OL counterpart, while any specific effect was observed in relation to the nature of the

polyelectrolyte layer, the performance of PDDA and CATLIG being similar. Note that the general efficacy of native HRP was decreased in the presence of VA (Table 2, entry 37 versus entry 11) and was only slightly increased with HoBt (Table 2, entry 38 versus entry 11), suggesting the benign effect of redox mediators in the desulfuration activity of HRP after the immobilization process.

The reusability of **cat X** was evaluated, as a representative sample, analyzing the oxidation of DBT for more runs. The experiment was performed by recovery of the biocatalyst and reuse for five runs under reported experimental conditions (Table 2, entries 32–36). As a general trend, **cat X** showed 45% conversion of substrate at the five run, suggesting the relative stability of the system.

3. Materials and Methods

3.1. Materials

Organosolv lignin (OL) and kraft lignin (KL) were obtained from chemical point and stora enso, respectively. Horseradish peroxidase (HRP, 173 U/mg), concanavalin A (ConA) from *Canavalia ensiformis* (Jack bean) type VI, poly(diallyldimethylammonium chloride) PDDA (20% *v/v* water solution), Bradford reagent, 2,2-azinobis-(3-ethylbenzothiazoline-6-sulfonic acid) (ABTS), hydrogen peroxide (H_2O_2, 35 wt%), dibenzothiophene (DBT), veratryl alcohol (VA),1-hydroxybenzotriazole (HoBt) from Sigma–Aldrich (St. Louis, MO, USA), were used without any further purification. Triplicate experiments with native and immobilized peroxidase were performed in Na-acetate buffer (0.1 M, pH 5.0) or phosphate buffer saline (PBS, 0.1 M, pH 8.0). Milli-Q water (ϱ = 18.2MΩ cm a 25 °C; TOC < 10 μg L^{-1}, Millipore, Molsheim, France) was used as solvent. CATLIG was prepared from kraft lignin (10 mg/ml; 0.1 M) in NaOH, by treatment with glycidyl tetramethyl ammonium chloride (20 mg) at 60 °C for 2 h under magnetic stirring. The crude was purified by dialysis with Spectrapore™ membrane (24 h, 3.5 kD MWCO). A Hewlett Packard 6890 with a FID (Flame ionization detector) and a 30 m × 0.32 mm × 0.25 mm column (cross-linked with 5% phenyl methyl siloxane) was used for the GC-MS determinations (He carrier gas). Mass-spectrometry was performed by 450 GC-320 MS apparatus (VARIAN, Palo Alto, CA, USA) by comparison with commercial samples. *n*-Hexadecane was used as internal standard. The product yield was referred to converted substrate.

3.2. Preparation of Cat I-II

A solution of organosolv lignin OL or kraft lignin (KL) (2.0 mg in 1.2 mL of THF/H_2O 5:1 v/v) was added to Milli-Q water (in 3.8 mL) to afford OL-LNPs and KL-LNPs [38]. Concanavalin A (0.5 mg) in PBS (1.0 mL, 0.1 M; pH 7.3) was added to OL-LNPs and KL-LNPs (1.5 mg) in PBS (1.0 mL) and the dispersion was sonicated for 5 min to yield OL/Con A and KL/Con A, followed by addition of HRP (0.1 mg, 18 U/mg) in PBS (0.1 mL, 0.1M; pH 7.3) under orbital shaking at 4 °C for 24 h. **Cat I-II** were isolated by centrifugation (20 min at 6000 rpm) and the residual solution was evaluated for the immobilization yield and activity parameters. Finally, **cat I-II** were washed with sodium phosphate buffer (1.0 mL, 0.1 M; pH 7.3) and lyophilized.

3.3. Preparation of Cat III-V and Cat IV-VI

Cat III and **V** carrying out PDDA as cationic polyelectrolyte were prepared in a similar way**.** OL-LNPs and KL-LNPs (15 mL Milli-Q water; 1.0 mg/mL, pH 4.2) were treated with PDDA (1.0 mg/mL, Milli-Q water) under magnetic stirring at 25 °C for 2 h. OL–PDDA or KL-PDDA intermediates were isolated by centrifugation and freeze dry. A PBS suspension (1.0 mL) of OL-PDDA and KL-PDDA (1.5 mg,) was treated with Concanavalin A (0.5 mg) in PBS (1.0 mL, 0.1 M; pH 7.3) and sonicated for 5 min to yield OL-PDDA/Con A and KL-PDDA/Con A, followed by addition of HRP (0.1 mg, 18 U/mg) in PBS (0.1 mL, 0.1M; pH 7.3) under orbital shaking at 4 °C for 24 h. **Cat III-V** were obtained by centrifugation (20 min at 6000 rpm) and the residual solution evaluated for the immobilization yield and activity parameters. **Cat III-V** were washed with PBS (1.0 mL, 0.1 M; pH 7.3) and lyophilized before the use. **Cat IV-VI** were prepared in a similar way, treating OL-LNPs and KL-LNPs (20 mg/mL, pH 4.2; Milli-Q water) with CATLIG (1 mg/mL, 15 mL; water solution) at 25 °C for 24 h to yield OL–CATLIG and KL-CATLIG intermediates. Next, these intermediates were

reacted with concanavalin A (0.5 mg) in PBS (1.0 mL, 0.1 M; pH 7.3) for 5 min, followed by addition of HRP (0.1 mg, 18 U/mg) in PBS (0.1 mL, 0.1M; pH 7.3) at 4 °C for 24 h to afford **cat V**-**VI** after centrifugation (20 min at 6000 rpm).

3.4. Preparation of Cat VII-X

In order to prepare **cat VII-IX** with PDDA-Con A/HRP as a double layer, the procedure described above was repeated under similar experimental conditions. Briefly, cat **III**-**V** in Milli-Q water (1.0 mL; 1.5 mg/mL) were treated with PDDA (1.0 mg/mL, water solution) at 4 °C for 2 h, followed by addition of concanavalin A (0.5 mg) in PBS (1.0 mL, 0.1 M; pH 7.3; for 1.0 h) and HRP (0.1 mg, 18 U/mg) in PBS (0.1 mL, 0.1M; pH 7.3) at 4 °C for 24 h, to yield **cat VII**-**IX** after centrifugation (20 min at 6000 rpm). **Cat VIII-X** were prepared by **cat IV-VI** (20 mg/mL, pH 4.2) to a CATLIG water solution (1.0 mg/mL, 15 mL) at 4 °C for 2 h, followed by addition of concanavalin A (0.5 mg) in PBS (1.0 mL, 0.1 M; pH 7.3) and HRP (0.1 mg, 18 U/mg) in PBS (0.1 mL, 0.1M; pH 7.3) at 4 °C for 24 h to afford **cat VIII**-**X** after centrifugation (20 min at 6000 rpm).

3.5. Scanning Electron Microscopy Analysis

The Field emission scanning electron microscopy (FESEM) (Carl Zeiss Microscopy GmbH) of **cat I-X** was acquired on FESEM ZEISS GeminiSEM500, operated at 5 kV after drop 20 µl (with deionized water) of biocatalyst dispersion on specimen stubs, air dried and coated with gold by sputtering with AGAR (Auto Sputter Coater). Before the observations, the sample received a deposition of chromium thin film (5 nm) by sputter coating using a QUORUM Q 150T ES plus coater.

3.6. Synthesis of FITC-Labeled HRP and Laser Confocal Microscopy

The procedure of fluorescent labelling of HRP was performed as described in literature. Briefly, HRP (20 mg) was solubilized in 4.0 mL of sodium bicarbonate buffer (pH 9.2, 50 mM). FITC (2mg) in 400 µL of dimethyl sulfoxide (DMSO) was added to HRP solution dropwise in the dark. Unreacted dye was removed through overnight dialysis using Spectra pore dialysis membrane (3.5 kD MWCO) against ammonium chloride (NH_4Cl). ZEISS LSM-710 NLO confocal system (Carl Zeiss Microscopy GmbH) equipped with a Plan Apochromat 100X/1.40 oil DIC M 27 objectives was used for laser confocal microscopy at the excitation wavelengths for FITC-HRP/Con A complex (488 nm).

3.7. ATR-IR Characterization

Lignin nanoparticles coated with Con A were analyzed by attenuated total reflection Fourier transform infrared (ATR-IR) spectroscopic (PerkinElmer Life and Analytical Sciences, Bridgeport Avenue,Milford, CT, USA) using a PerkinElmer (Spectrum One) spectrometer (UATR unit cell) averaging 32 scans (resolution of 4 cm^{-1}).

3.8. Activity Parameters of Cat I-X

The ABTS test was used for the determination of the enzymatic activity of HRP and **cat I-X** [50] by following the cation radical absorption (sodium acetate buffer solution, 0.1 M, pH 5, 3.0 mL) at 415 nm ($\varepsilon 420$ = 36 000 M^{-1} cm^{-1}) at different concentrations of HRP. In a typical experiment, the appropriate biocatalyst (18 U in acetate buffer solution, 0.1 M, pH 5, 3.0 mL), corresponding to c.a. 1.0 mg of LNPs), was added to a acetate buffer solution (0.5 mM) of ABTS and 0.3% of H_2O_2. One unit activity of HRP is the amount of enzyme that transforms 1.0 µmole of H_2O_2 per minute at pH 5 at 25 °C.

3.9. Kinetic Data of Cat I-X

Kinetic data (K_m and V_{max}) were collected by using different concentrations of ABTS (0.3–20 mM) in sodium acetate buffer (pH 5) with HRP concentration (18 U) and H_2O_2 dose (0.3%) kept constant. Lineweaver–Burk plots furnished the initial velocities (1/V vs. 1/[S]), K_m and V_{max} being calculated as

intercepts at the cartesian axes, respectively. Kinetic data were analyzed by GraphPad software in triplicate, using native and immobilized HRP.

3.10. Oxidation of DBT with cat I-X and Redox Mediator Systems.

As a general procedure, DBT (10 mg) was dissolved in a solution of *n*-hexane (4 ml) and PBS (0.1M pH 8, 4mL) and left under magnetic stirring. The appropriate amount (18 U/mg) of Cat (**I-X**) were added to the biphasic dispersion, that was heated at 45 °C and H_2O_2 (4.0 equiv) was added in seven steps to avoid the inactivation of HRP [26]. In alternative, the oxidation of DBT was performed with HoBt and VA as redox mediators. The formation of DBTO in the polar phase was monitored by thin layer chromatography (TLC, n-hexane/EtOAc = 3.0:7.0). The reaction was conducted for two hours, after this time, **cat I-X** were centrifuged (6000 rpm) for 20 min and the buffer and organic layers were analyzed by gas-chromatography associated to mass-spectrometry (GC-MS) (VARIAN, Palo Alto, CA, USA))in order to evaluate the conversion of DBT. Next, the polar phase was evaporated under reduced pressure and DBTO was collected and analyzed by GC-MS. LNPs alone were unreactive.

4. Conclusions

In conclusions, nanoparticles of lignin are effective functional and natural platforms for the immobilization of the HRP/Con A complex. In this process, the hydrophobicity of the support was a crucial parameter, OL favoring the dissociation of Con A into the two un-effective sub-unit components. In this context, hydrophilic KL was the most efficient support. Thanks to the selective supramolecular interaction between Con A and the oligosaccharide part of HRP, that is located far from the active site of the enzyme, the overall activity of the system was generally retained after the immobilization. The presence of the cationic polyelectrolyte layer increased the overall stability and activity of the biocatalyst, PDDA and CATLIG showing a similar behavior. Moreover, multilayered systems performed better than the single layered counterpart, confirming the beneficial effect of the layered structure in preserving the enzyme from possible denaturation processes. On the other hand, some mass-transfer limitation occurred in the biphasic medium PBS/*n*-hexane during the oxidation of DBT. This kinetic limitation was solved through the use of VA and HoBt, that enhanced the efficacy of the biocatalyst acting as redox shuttles between the active site of HRP and the bulk of the solution. HoBt performed better then VA in accordance with the previously reported lower value of the internal redox potential that make this molecule significantly more reactive toward DBT by hydrogen atom abstraction mechanism [59]. Irrespective from the experimental conditions, DBTO was obtained as the only recovered product, highlighting the high reactivity and selectivity of HRP and making easier the successive extraction of the polar end product from the oil phase. The possibility of removing DBT with efficacy similar to native HRP (65%), associated to the general green property of the system, relative low operative reaction temperature (45 °C), room pressure and recyclability, makes HRP/Con A lignin biocatalysts effective new entries in bio-desulfurization ODS processes. Among the most active biocatalysts, **cat X** that is composed only by renewable, biocompatible and biodegradable materials (KL, Con A and CATLIG) is a real full green alternative for ODS in sustainable circular economy scenarios.

Author Contributions: D.P., E.C. and B.M.B synthesized and characterized the catalysts and analyzed the kinetic and activity data of the catalysts**.** R.S.; E.C. and L.B. designed the experiments and wrote the paper**.** M.C. contributed to FTIR analysis and SEM characterization. All authors have read and agreed to the published version of the manuscript.

Funding: This work was supported by the EU project- EASME/EMFF/Blue Economy-2018/n.863697 "FISH chitinolytic biowastes FOR FISH active and sustainable packaging material" (FISH4FISH)".

Acknowledgments: Lorenzo Arrizza and Microscopies center of L'Aquila University are acknowledged for SEM analyses and the Large Equipment Center (CGA) of Tuscia University are acknowledged for confocal analysis.

Conflicts of Interest: The authors declare no conflict of interest.

References

1. De Souza, W.F.; Guimaraes, I.; Guerreiro, M.C.; Oliveira, L.C.A. Catalytic oxidation of sulfur and nitrogen compounds from diesel fuel. *Appl. Catal. A General* **2009**, *360*, 205–209.
2. Zannikos, F.; Lois E.; Stournas, S. Desulfurization of petroleum fractions by oxidation and solvent extraction. *Fuel Process. Technol.* **1995**, *42*, 35–45.
3. Ismagilov, Z.; Yashnik, S.; Kerzhentsev, M.; Parman, V.; Bourane, A.; Al-Shahrani, F.M.; Haji, A.A.; Koseoglu, O.R. Oxidative desulfurization of hydrocarbon fuels. *Catal. Rev. Sci. Eng.* **2011**, *53*, 199–255.
4. Gatan, R.; Barger, P.; Gembicki, V.; Cavanna, A.; Molinari, D. Oxidative desulfurization: a new technology for ULSD. *Am. Chem. Soc. Div. Fuel Chem*. **2004**, *49*, 577–579.
5. Li, J.; Yang, Z.; Li, S.; Jin, Q.; Zhao, J. Review on oxidative desulfurization of fuel by supported heteropolyacid catalysts *J. ind.eng. chem.* **2020**, *82*, 1–16.
6. Hossain, M.N.; Park, H.C.; Choi, H.S. A comprehensive review on catalytic oxidative desulfurization of liquid fuel oil. *Catalysts* **2019**, *9*, 229.
7. Crucianelli, M.; Bizzarri, B.M.; Saladino R. SBA-15 Anchored Metal Containing Catalysts in the Oxidative Desulfurization Process. *Catalysts* **2019**, *9*, 984–1015.
8. Houda, S.; Lancelot, C.; Blanchard, P.; Poinel, L.; Lamonier, C. Oxidative desulfurization of heavy oils with high sulfur content: A review. *Catalysts* **2018**, *8*, 344.
9. Sikarwar, P.; Gosu, V.; Subbaramaiah, V. An overview of conventional and alternative technologies for the production of ultra-low-sulfur fuels. *Rev. Chem. Eng.* **2019**, *35*, 669–705.
10. Mjalli, F.S.; Ahmed, O.U.; Al-Wahaibi, T.; Al-Wahaibi, Y.; Al-Nashef, I.M. Deep oxidative desulfurization of liquid fuels. Rev. Chem. Eng. **2014**, *30*, 337–378.
11. Saladino, R.; Botta, G.; Crucianelli, M. Advances in Nanostrostructured Transition Metal Catalysis Applied to Oxidative Desulfurization. Applying Nanotechnology to the Desulfurization Process in Petroleum Engineering, Tawfik A. Saleh (Ed.), IGI Global: Hershey, PA, USA, 2016; pp.180-215.
12. Piccinino D.; Abdalghani I.; Botta G.; Crucianelli M.; Passacantando M.; Di Vacri, M.L.; Saladino R. Preparation of wrapped carbon nanotubes poly(4-vinylpyridine)/MTO based heterogeneous catalysts for the oxidative desulfurization (ODS) of model and synthetic diesel fuel. *Appl. Catal. B-Environ*. **2017**, *200*, 392–401.
13. Di Giuseppe, A.; Crucianelli, M.; De Angelis, F.; Crestini, C.; Saladino, R. Efficient Oxidation of Thiophene Derivatives with Homogeneous and Heterogeneous MTO/H_2O_2 systems: a novel approach for Oxidative Desulfurization (ODS) of Diesel Fuel. *Appl.Catal. B-Environ*. **2009**, *89*, 239–245.
14. Davoodi-Dehaghania, F.; Vosoughi, M.; Ziaee, A.A. Biodesulfurization of dibenzothiophene by a newly isolated Rhodococcus erythropolis strain. *Bioresour. Technol*. **2010**, *101*, 1102–1105.
15. Wang, P.; Humphrey, A.E.; Krawiec, S. Kinetic Analyses of Desulfurization of Dibenzothiophene by Rhodococcus erythropolis in Continuous Cultures. *Appl. Environ. Microbiol.* **1996**, *62*, 3066–3068.
16. Chang, J.H.; Chang, Y.K.; Cho, K.; Chang, H.N.; Desulfurization of model and diesel oils by resting cells of Gordona sp. *Biotechnol. Lett*. **2000**, *22*, 193–196.
17. Villaseňor, F.; Loera, O.; Campero, A.; Viniegra-Gonzàlez, G. Oxidation of dibenzothiophene by laccase or hydrogen peroxide and deep desulfurization of diesel fuel by the later. *Fuel Process. Technol.* **2004**, *86*, 49–59.
18. Bressler, D.C.; Fedorak, P.M.; Pickard, M.A. Oxidation of carbazole, N-ethylcarbazole, fluorene, and dibenzothiophene by the laccase of Coriolopsis gallica. *Biotechnol. Letters* **2000**, *14*, 1119–1125.
19. Klyachko, N.L.; Klibanov, A.M.; Oxidation of dibenzothiophene catalyzed by hemoglobin and other hemoproteins in various aqueous– organic media. *Appl. Biochem. Biotechnol*. **1992**, *37*, 53–68.
20. Vazquez-Duhalt, R.; Westlake, D.W.S.; Fedorak, P.M. Lignin Peroxidase Oxidation of Aromatic Compounds in Systems Containing Organic Solvents. *Appl. Env. Micr.* **1994**, *60*, 459–466.
21. Eibes, G.; Cajthaml, T.; Moreira, M.T. Feijoo, J.; Lema, J.M. Enzymatic degradation of anthracene, dibenzothiophene and pyrene by manganese peroxidase in media containing acetone. *Chemosphere* **2006**, *64*, 408–414.
22. Ichinose, H.; Wariishi, H.; Tanaka, H. Effective oxygen transfer reaction catalyzed by microperoxidase-11 during sulfur oxidation of dibenzothiophene. *Enzyme Microb. Technol.* **2002**, *30*, 334–339.
23. Ayala, M.; Tinoco, R.; Hernandez, V.; Bremauntz, P.; Vazquez-Duhalt, R. Biocatalytic oxidation of fuel as an alternative to biodesulfurization. *Fuel Process. Technol*. **1998,** *57*, 101–111.

24. Doerge, D.R.; Cooray, N.M.; Brewster, M.E. Peroxidase-catalyzed S-oxygenation: mechanism of oxygen transfer for lactoperoxidase. *Biochemistry* **1991**, *30*, 8960.
25. Stachyra, T.; Guillochon, D.; Pulvin, S.; Thomas, D. Hemoglobin, horseradish peroxidase, and heme-bovine serum albumin as biocatalyst for the oxidation of dibenzothiophene. *Appl. Biochem. Biotech.* **1996**, *59*, 231–244.
26. Da Silva Madeira, L.; Ferreira-Leitaŏ, V.S.; da Silva Bon, E.P. Dibenzothiophene oxidation by horseradish peroxidase in organic media: Effect of the DBT:H_2O_2 molar ratio and H_2O_2 addition mode. *Chemosphere* **2008**, *71*, 189–194.
27. Bhasarkar, J.; Borah, A.J.; Goswami, P.; Moholkar, V.S. Mechanistic analysis of ultrasound assisted enzymatic desulfurization of liquid fuels using horseradish peroxidase. *Bioresour. Technol.* **2015**, *196*, 88–98.
28. Ayala, M.; Verdin, J.; Vazquez-Duhalt, R. The prospects for peroxidase-based biorefining of petroleum fuels. *Biocatal. Biotransform.* **2007**, *25*, 114–129.
29. Terrès, E.; Montiel, M.; Le Borgne, S.; Torres, E. Immobilization of chloroperoxidase on mesoporous materials for the oxidation of 4,6-dimethyldibenzothiophene, a recalcitrant organic sulfur compound present in petroleum fractions. *Biotechnol. Lett*. **2008**, *30*, 173–179.
30. Wu, S.; Lin, J.; Chan, S. Oxidation of dibenzothiophene catalyzed by heme-containing enzymes encapsulated in sol-gel glass. *Appl. Biochem. Biotechnol.* **1994**, *47*, 11–20.
31. Li, Y.; Huang, X.; Qu, Y. A strategy for efficient immobilization of laccase and horseradish peroxidase on single-walled carbon nanotubes. *J. Chem. Technol. Biotechnol.* **2013**, *88*, 2227–2232.
32. Juarez-Moreno, K.; Díaz de León, J.N.; Zepeda, T.A.; Vazquez-Duhalt, R.; Fuentes, S. Oxidative transformation of dibenzothiophene by chloroperoxidase enzyme immobilized on (1D)-γ-Al_2O_3 nanorods. *J. Mol. Catal. B-enzym.* **2015**, *115*, 9095.
33. Mateo, C.; Palomo, J.M.; Fernandez-Lorente, G.; Guisan, J.M.; Fernandez-Lafuente, R. Improvement of enzyme activity, stability and selectivity via immobilization techniques. *Enzyme Microb. Technol.* **2007**, *40*, 1451–1463.
34. Hu, T.Q. *Chemical Modification, Properties, and Usage of Lignin;* Kluwer Academic-Plenum Publishers: New York, NY, USA, **2002.**
35. Piccinino, D.; Capecchi, E.; Botta, L.; Bizzarri, B.M.; Bollella, P.; Antiochia, R.; Saladino, R. Layer-by-Layer Preparation of Microcapsules and Nanocapsules of Mixed Polyphenols with High Antioxidant and UV-Shielding Properties. *Biomacromolecules*, **2018**, *19*, 3883–3893.
36. Capecchi, E.; Piccinino, D.; Bizzarri, B.M.; Avitabile, D.; Pelosi, C.; Colantonio, C.; Calabrò, G.; Saladino, R. Enzyme-Lignin Nanocapsules Are Sustainable Catalysts and Vehicles for the Preparation of Unique Polyvalent Bioinks. *Biomacromolecules* **2019**, *20,* 1975–1988.
37. Capecchi, E.; Piccinino, D.; Delfino, I.; Bollella, P.; Antiochia, R.; Saladino, R. Functionalized tyrosinase-lignin nanoparticles as sustainable catalysts for the oxidation of phenols. *Nanomaterials* **2018**, *6*, 438.
38. Piccinino, D.; Capecchi, E.; Botta, L.; Bollella, P.; Antiochia, R.; Crucianelli, M.; Saladino, R. Layer by layer supported laccase on lignin nanoparticles catalyzes the selective oxidation of alcohols to aldehydes. *Catal. Sci. Technol.* **2019**, 9, 4125–4134.
39. Frommhagen, M.; Mutte, S.K.; Westphal, A.H.; Koetsier, M.J.; Hinz, S.W.A.; Visser, J.; Vincken, J.P.; Weijers, D.; Van Berkel, W.J.H.; Gruppen, H.; Kabel, M.A. Boosting LPMO-driven lignocellulose degradation by polyphenol oxidase-activated lignin building blocks. *Biotechnol. Biofuels* **2017**, *10*, 121.
40. Brenelli, L.; Squina, F.M.; Felby, C.; Cannella, D. Laccase-derived lignin compounds boost cellulose oxidative enzymes AA9. *Biotechnol. Biofuels*, **2018**, *11*, 10.
41. Ortiza, E.; Gallay, P.; Galicia, L.; Eguílaz, M.; Rivas, G. Nanoarchitectures based on multi-walled carbon nanotubes non-covalently functionalized with Concanavalin A: A new building-block with supramolecular recognition properties for the development of electrochemical biosensors. *Sens. and Actuators B: Chem.* **2019**, *292*, 254–262.
42. Ferreira, J.A.; Taherzadeh, M.J. Improving the economy of lignocellulose-based biorefineries with organosolv pretreatment. *Biores. Technol*. **2020**, *299*, 122.
43. Demuner I.F.; Colodette J.L.; Demuner A.J.; Jardim C.M. Biorefinery review: Wide-reaching products through kraft lignin. *Bioresources* **2019**, *14*, 7543–7581.
44. Leskinen, T.; Smyth, M.; Xiao, Y.; Lintinen, K.; Mattinen, M.L.; Kostiainen, M.A.; Oinas, P.; Österberg, M. Scaling Up Production of Colloidal Lignin Particles. *Nord. Pulp Pap. Res. J.* **2017**, *32*, 586.

45. Liu, Y.; Yu. J. Oriented immobilization of proteins on solid supports for use in biosensors and biochips: a review. *Microchim. Acta.* **2016**, *183*, 1–19.
46. Makky, A.; Michel, J.P.; Maillard, P.; Rosilio V. Biomimetic liposomes and planar supported bilayers for the assessment of glycodendrimeric porphyrins interaction with an immobilized lectin. *Biochim. Biophys. Acta. Rev. Biomembr.* **2011**, *1808*, 656–666.
47. Zhang, Y.; Yong, Y.; Ge, J.; Liu, Z. Lectin agglutinated multienzyme catalyst with enhanced substrate affinity and activity. *ACS Catal.* **2016**, *6*, 3789–3795.
48. Huang, J.; Zhuang, W.; Wei, C.; Mu, L.; Zhu, J.; Zhu, Y.; Jinglan, W.; Yong, C.; Ying, H. Concanavalin A induced orientation immobilization of Nuclease P1: The effect of lectin agglutination. *Process Biochem.* **2018**, *64*, 160–169.
49. Yong, Y.; Su, R.; Liu, X.; Xu, W.; Zhang, Y.; Wang, R.; Ouyang, P.; Wu, J.; Ge, J.; Liu, Z. Lectin corona enhances enzymatic catalysis on the surface of magnetic nanoparticles. *Biochem. Eng. J.* **2018**, *129*, 26–32.
50. Saladino, R.; Guazzaroni, M.; Crestini, C.; Crucianelli, M. Dye Degradation by Layer-by-Layer Immobilised Peroxidase/Redox Mediator Systems. *ChemCatChem* **2013,** *5*, 1407–1415.
51. Xu, X.; Yuan, Y.; Guixian, H.; Wang X.; Qi, P.; Wang, Z.; Wang, Q.; Wang, X.; Fu, Y.; Li, Y.; Yang, H. Exploiting pH-Regulated Dimer- Tetramer Transformation of Concanavalin A to Develop Colorimetric Biosensing of Bacteria. *Sci. Rep.* **2017**, *7*, 2045–2322.
52. Xu, W.; Yong, Y.; Wang, Z.; Jiang, G.; Wu, J.; Liu, Z. Concanavalin A Coated Activated Carbon for High Performance Enzymatic Catalysis. *ACS Sustainable Chem. Eng.* **2017**, *5*, 90–96.
53. Palazzo, G.; Colafemmina, G.; Guzzoni Iudice, C.; Mallardi, A. Three immobilized enzymes acting in series in layer by layer assemblies: Exploiting thetrehalase-glucoseoxidase-horseradish peroxidase cascade reactions for the optical determination of trehalose. *Sens. Actuators B chem.* **2014**, *202*, 217–223.
54. Rong, J.; Zhou, Z.; Wang, Y.; Han, J.; Li, C.; Zhang, W.; Ni, L. Immobilization of Horseradish Peroxidase on Multi-Armed Magnetic Graphene Oxide Composite: Improvement of Loading Amount and Catalytic Activity. *Food Technol. Biotech.* **2019**, *57*, 1330–1334.
55. Zhang, F.; Wang, M.; Liang, C.; Jiang, H.; Shen, J.; Li, H. Thin-Layer Polymer Wrapped Enzymes Encapsulated in Hierarchically Mesoporous Silica with High Activity and Enhanced Stability. *Sci. Rep.* **2014**, *4*, 4421.
56. Tischer, W. Immobilized enzymes: Crystals or carriers? *Trends Biotechnol*. **1999**, *117*, 326–335.
57. Won, K.; Kim, Y.H.; An, E.S.; Lee, Y.S.; Song, B.K. Horseradish Peroxidase-Catalyzed Polymerization of Cardanol in the Presence of Redox Mediators. *Biomacromolecules* **2004**, *5*, 1–4.
58. Razola, S.S.; Aktas, E.; Viré, J.-C.;Kauffmann, J.-M. Reagentless enzyme electrode based on phenothiazine mediation of horseradish peroxidase for subnanomolar hydrogen peroxide determination. *Analyst* **2000**, *125*, 79–85.
59. Baciocchi, E.; Gerini, M.F.; Lanzalunga, O.; & Mancinelli, S. Lignin peroxidase catalysed oxidation of 4-methoxymandelic acid. The role of mediator structure. *Tetrahedron* **2002**, *58*, 8087–8093.